Giant forced-volume and saturation magnetostrictions of amorphous $La(Fe_xAl_{1-x})_{13}$ alloys composed of icosahedral clusters

1995 J. Phys.: Condens. Matter 7 2875

(http://iopscience.iop.org/0953-8984/7/14/024)

J. Phys.: Condens. Matter 7 (1995) 2875–2887. Printed in the UK

Giant forced-volume and saturation magnetostrictions of amorphous $La(Fe_xAl_{1-x})_{13}$ alloys composed of icosahedral clusters

K Fukamichi†, T H Chiang†§, A Fujita†, H Tange‡, S Kawabuchi‡ and T Ono‡

† Department of Materials Science, Faculty of Engineering, Tohoku University, Sendai 980, Japan

‡ Department of Physics, Faculty of Science, Ehime University, Matsuyama 790, Japan

Received 1 July 1994

Abstract. The dependences of saturation magnetostriction λ_s and forced-volume magnetostriction $\partial\omega/\partial H$ on the concentration and temperature have been investigated for amorphous $La(Fe_xAl_{1-x})_{13}$ alloys prepared by high-rate DC sputtering. The magnetic phase diagram obtained from the differential magnetic susceptibility dM/dH has been correlated with these magnetostrictions.

The spin freezing temperature T_f is drastically decreased but the Curie temperature T_C is slightly increased on application of a magnetic field. The temperature dependences of λ_s and $\partial\omega/\partial H$ exhibit a broad peak at the spin freezing temperature T_f. The temperature dependence of λ_s for the ferromagnetic alloys is explained by the two-ion model, reflecting the peculiar amorphous structure consisting of icosahedral clusters. The peak of $\partial\omega/\partial H$ at the Curie temperature becomes indistinct with increasing ferromagnetic state in contrast with the peak at the spin freezing temperature. The giant values of $\partial\omega/\partial H$ and its divergent behaviour at the spin freezing temperature are accounted for by the variable amplitude of the local magnetic moment in the itinerant spin glasses.

The significant large $\partial\omega/\partial H$ is connected with the pronounced large magnetovolume and magnetoelastic effects such as the spontaneous volume magnetostriction ω_s, compressibility κ and high-field susceptibility χ_{hf} which bring about various Invar anomalies.

1. Introduction

Crystalline $La(Fe_xAl_{1-x})_{13}$ compounds are formed in the concentration range $0.46 \leqslant x \leqslant 0.92$ (Palstra *et al* 1984) and their magnetic properties have been investigated extensively (Palstra *et al* 1984, 1985, 1986, Helmholdt *et al* 1986, Ludorf *et al* 1989). It has been reported that the magnetic state is sensitively influenced by x and the compound with $x = 0.91$ is antiferromagnetic (Helmholdt *et al* 1986). These compounds have a cubic $NaZn_{13}$ type of structure containing separated icosahedra composed of Fe and Al atoms (Palstra *et al* 1984). The icosahedral structure has often been closely correlated to the structures of amorphous and quasicrystalline alloys (Kofart *et al* 1986, Widom 1988).

The existence of icosahedral clusters in amorphous $La(Fe_xAl_{1-x})_{13}$ $(0.80 \leqslant x \leqslant 0.95)$ alloys has been confirmed by x-ray diffraction analysis (Matsubara *et al* 1992). The data on the isomer shift and quadrupole splitting for the crystalline and amorphous $La(Fe_{0.9}Al_{0.1})_{13}$ alloys (Chiang *et al* 1994) have the same values, being consistent with the x-ray analysis

§ Present address: TDSC Co. Ltd, 13F-7 No 398 Hwang-Pei Road, Chung-Li, Taiwan.

0953-8984/95/142875+13$19.50

mentioned above. The amorphous alloys exhibit re-entrant spin-glass behaviour in the concentration range $0.85 < x \leqslant 0.95$ (Chiang *et al* 1991), although the crystalline counterparts are antiferromagnetic (Palstra *et al* 1985). The ferromagnetic state is stabilized below $x = 0.85$ in the amorphous alloys (Chiang *et al* 1991). The nearest-neighbour configuration of Fe sites is very similar to that in γ-Fe. The atomic distance of the Fe–Fe nearest neighbours in both crystalline and amorphous states is about 2.55 Å (Ludorf *et al* 1989, Matsubara *et al* 1992, Chiang *et al* 1994). This value is very close to the critical distance for the transition from the ferromagnetic to antiferromagnetic state (Ludorf *et al* 1989). In such circumstances, a pronounced thermal expansion anomaly associated with the Invar effect is observed in both states (Palstra *et al* 1985, Chiang *et al* 1992). The compressibility κ obtained from data on the Brillouin scattering is extremely large (Yoshihara *et al* 1994). Large values of the spontaneous volume magnetostriction ω_s and the high-field susceptibility χ_{hf} in the crystalline and amorphous states have been reported (Palstra *et al* 1985, Chiang *et al* 1991, 1992). These results are closely relevant to the Invar effects (Shiga 1992). Because $\partial\omega/\partial H$ is proportional to the high-field susceptibility χ_{hf}, a large value of $\partial\omega/\partial H$ is expected in the present amorphous alloys.

The Invar effects are common to Fe-based amorphous alloys (Fukamichi 1983). Amorphous Zr–Fe alloys exhibit large thermal expansion and elastic anomalies (Fukamichi *et al* 1984, 1989) and these alloys show re-entrant spin-glass behaviour (Hiroyoshi and Fukamichi 1982, Fukamichi *et al* 1989). The temperature dependence of the giant forced-volume magnetostriction $\partial\omega/\partial H$ for the amorphous Zr–Fe alloys has been confirmed (Tange *et al* 1989, 1990) and theoretically discussed using the Liberman–Pettifor formula, taking into account the thermal spin fluctuations (Kakehashi 1993). On the other hand, it has been pointed out that the saturation magnetostriction λ_s of amorphous Fe-based alloys is proportional to the square of the magnetization except at low temperatures (O'Handley 1977), which is accounted for by the single-ion model (Callen and Callen 1963, 1965). The magnetization of the present amorphous alloys is large, ranging from about 140 to 170 emu g^{-1} at 4.2 K (Chiang *et al* 1991).

Large values of the saturation and forced-volume magnetostrictions are expected for the amorphous $La(Fe_xAl_{1-x})_{13}$ alloys. In the present paper, therefore, the dependences of the saturation magnetostriction λ_s and the forced-volume magnetostriction $\partial\omega/\partial H$ on the concentration and temperature have been investigated. The magnetic phase diagram in an applied magnetic field is obtained by measuring the differential magnetic susceptibility at various magnetic field strengths. These data will be connected with the spin-glass and ferromagnetic states. Furthermore, the iterant-electron spin-glass behaviour will be discussed.

2. Experimental details

The alloy targets for sputtering were made by arc melting in an argon gas atmosphere. Several amorphous $La(Fe_xAl_{1-x})_{13}$ ($0.80 \leqslant x \leqslant 0.95$) samples about 0.3 mm thick were prepared by high-rate DC sputtering on a water-cooled Cu substrate. The Cu substrate was dissolved in dilute chromic acid kept at about 350 K. Their amorphous state was confirmed by x-ray diffraction.

In order to obtain the magnetic transition temperatures, the magnetization was measured between 4.2 and 300 K in various magnetic fields up to 1 kOe with a SQUID magnetometer, and the differential magnetic susceptibility was calculated numerically from the adjoining two points of the magnetization curves measured at each temperature. Measurements of the saturation magnetostriction λ_s and the forced-volume magnetostriction $\partial\omega/\partial H$ were carried out by a three-terminal capacitance method at temperatures 4.2–300 K in magnetic fields up to 16 kOe.

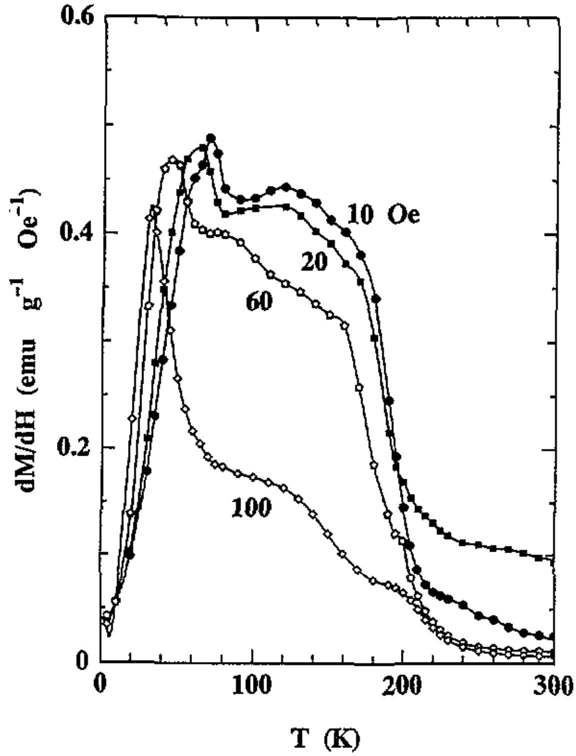

Figure 1. Temperature dependence of the differential magnetic susceptibility dM/dH measured below 100 Oe for the amorphous $La(Fe_{0.95}Al_{0.05})_{13}$ alloy.

3. Results and discussion

A magnetic phase diagram of the temperature versus magnetic field is necessary to discuss the forced-volume magnetostriction. The temperature dependence of differential magnetic susceptibility dM/dH of the amorphous $La(Fe_{0.95}Al_{0.05})_{13}$ alloy obtained at various DC fields is shown in figure 1. The dM/dH curve measured in a field of 10 Oe shows two peaks. This means that the spin-glass transition proceeds through two steps, i.e. the higher temperature T_g of the freezing temperature of transverse component of spins and the lower temperature T_f of the freezing temperature of longitudinal spin components (Fujita *et al* 1993). With increasing external magnetic field, both T_f and T_g shift to lower temperatures and the former peak becomes sharp but the latter peak becomes uncertain. On further increase in the magnetic field, T_g disappears and a third broad peak appears at around 200 K. This temperature is regarded as the Curie temperature T_C because it corresponds to the inflection point of the thermomagnetization curve measured in the same magnetic field in analogy with the behaviour of Y–Fe amorphous alloys (Fujita *et al* 1993). As seen from figure 2, this third peak shifts slightly to higher temperatures with increasing applied magnetic field. From these results, the freezing temperatures and the Curie temperatures versus the external magnetic field are obtained for the amorphous $La(Fe_{0.95}Al_{0.05})_{13}$ and $La(Fe_{0.90}Al_{0.10})_{13}$ alloys as shown in figure 3. A similar result for the amorphous $La(Fe_{0.8}Al_{0.2})_{13}$ alloy which has no spin-glass behaviour is given in figure 4. With increasing applied magnetic field strength, the peak corresponding to the Curie temperature increases slightly. Therefore, it should be emphasized that T_g and T_f are drastically decreased by relatively low magnetic fields, whereas T_C is slightly increased on application of a magnetic field.

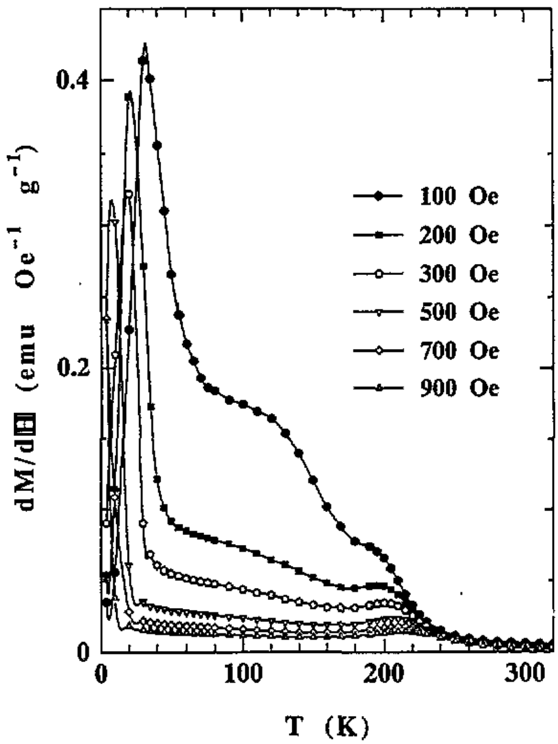

Figure 2. Temperature dependence of the differential magnetic susceptibility dM/dH measured above 100 Oe for the amorphous $La(Fe_{0.95}Al_{0.05})_{13}$ alloy.

Figures 5 and 6 show the longitudinal and transverse linear magnetostrictions for four amorphous $La(Fe_xAl_{1-x})_{13}$ alloys measured at 4.2 K and 77 K, respectively. The directions of the arrows in figure 5 indicate the increasing and decreasing applied magnetic fields. The point to note is that the magnetostrictions $\lambda_\parallel$ and $\lambda_\perp$ of both directions at 4.2 K for the alloys with $x = 0.95$ and 0.90 do not return to the starting point when the applied magnetic field is decreased. This behaviour is caused by the magnetic viscosity which is characteristic of spin-glass alloys, and it disappears at 77 K as seen from figure 6. That is, the spin-glass state occurs at 4.2 K, and the ferromagnetic state at 77 K, in accordance with figure 3. The temperature dependence of the magnetic viscosity will be referred to later in the discussion of figure 10. The magnetostrictions of both directions are almost saturated above 5 kOe for $x = 0.80$ and 0.85. On the other hand, the curves for $x = 0.90$ and 0.95 are not saturated. In the present study, the saturation magnetostriction $\lambda_\parallel$ for the latter has been obtained by linear extrapolation from the high-field ranges.

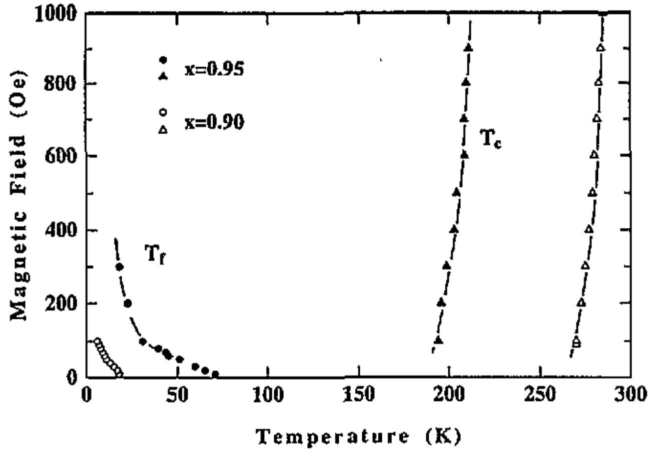

Figure 3. The magnetic phase diagrams for the amorphous La(Fe$_{0.95}$Al$_{0.05}$)$_{13}$ and La(Fe$_{0.90}$Al$_{0.10}$)$_{13}$ alloys in the magnetic field: ●, ○, spin freezing temperature T_f; ▲, △, Curie temperature T_C.

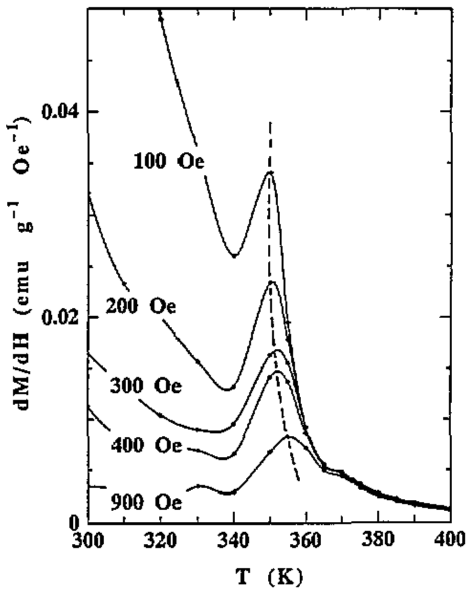

Figure 4. Temperature dependence of the differential magnetic susceptibility dM/dH for the amorphous La(Fe$_{0.80}$Al$_{0.20}$)$_{13}$ alloy: – – –, shift in the Curie temperature with the external magnetic field strength.

Figure 7 shows the temperature dependence of the saturation magnetization λ_s for the ferromagnetic amorphous alloys with $x = 0.85$ and 0.80. These amorphous alloys exhibit a monotonic variation with temperature, but the re-entrant spin-glass alloys with $x = 0.90$ and 0.95 exhibit a broad maximum at the spin freezing temperature, as seen from figure 8. Shown in figure 9 is the concentration dependence of the saturation magnetostriction λ_s measured at 4.2 K in a field of 10 kOe. A maximum of about 26×10^{-6} is observed at

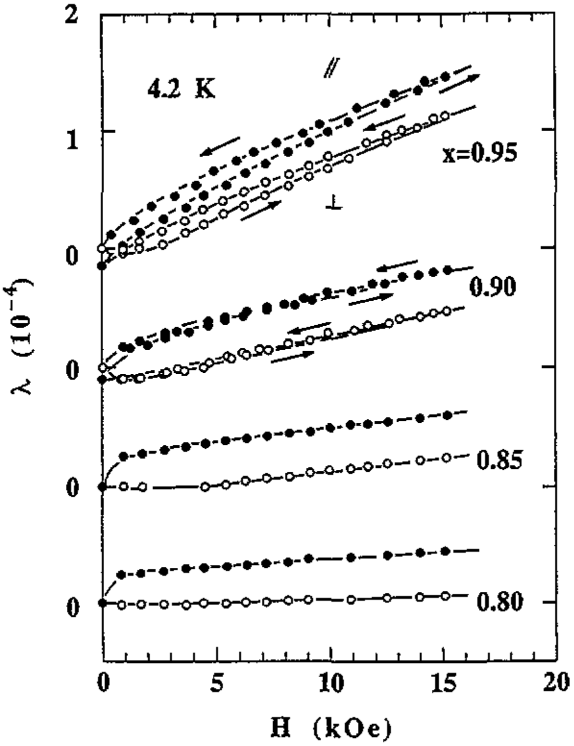

Figure 5. The field dependences of the longitudinal magnetostriction $\lambda_{\parallel}$ (–●–) and the transverse magnetostriction $\lambda_{\perp}$ (–○–) at 4.2 K for amorphous $La(Fe_xAl_{1-x})_{13}$ alloys. The directions of the arrows indicate the increasing and decreasing applied magnetic fields.

$x = 0.85$, i.e. the value of λ_s increases with increasing Fe content within the concentration of the ferromagnetic state, whereas it decreases in the regime of the spin-glass state. The temperature dependence of λ_s has been accounted for using one- or two-ion models (Callen and Callen 1963, 1965, O'Handley 1978) and the temperature is often converted to the corresponding magnetization. It has been pointed out that λ_s for amorphous Fe_xB_{1-x} ($0.78 \leqslant x \leqslant 0.86$) and $Fe_{0.75}P_{0.15}C_{0.10}$ alloys is expected to scale as the square M^2 of the magnetization except at low temperatures (O'Handley 1977, Berry and Pritchet 1978) in accordance with the single-ion model (Callen and Callen 1965). Note that the one-ion model seems to show a linear relationship in limited temperature ranges. The concentration dependence of the square M^2 of the magnetization measured at the same applied magnetic field strength is also plotted in the same figure. The curve of λ_s exhibits a similar tendency to M^2. On the other hand, the two-ion model shows that λ_s is proportional to the square M^2 of the magnetization throughout the entire temperature range up to the Curie temperature T_C. In figure 10, λ_s versus M^2 plots for the amorphous $La(Fe_{0.80}Al_{0.20})_{13}$ ferromagnetic alloy are given in order to make the difference between these models clear. The one-ion and two-ion models are shown as a broken curve and a solid line, respectively. The data for $La(Fe_{0.80}Al_{0.20})_{13}$ are on the solid line. Therefore, the present results are explicable by the two-ion model (Callen and Callen 1963, 1065). In the $NaZn_{13}$-type crystalline compounds $La(Fe_xAl_{1-x})_{13}$, there are two Fe sites in the icosahedral clusters, namely Fe^I and Fe^{II}. The Fe^I atoms are surrounded by an icosahedron of 12 Fe^{II} composed of Fe and Al atoms, depending on x. The Fe^{II} atoms are surrounded by the nine nearest Fe^{II} atoms and one

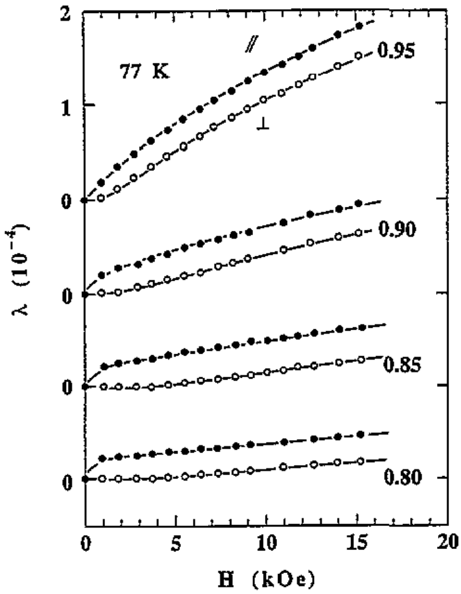

Figure 6. The field dependences of the longitudinal magnetostriction $\lambda_{\parallel}$ (–●–) and the transverse magnetostriction $\lambda_{\perp}$ (–○–) at 77 K for the amorphous La(Fe$_x$Al$_{1-x}$)$_{13}$ alloys.

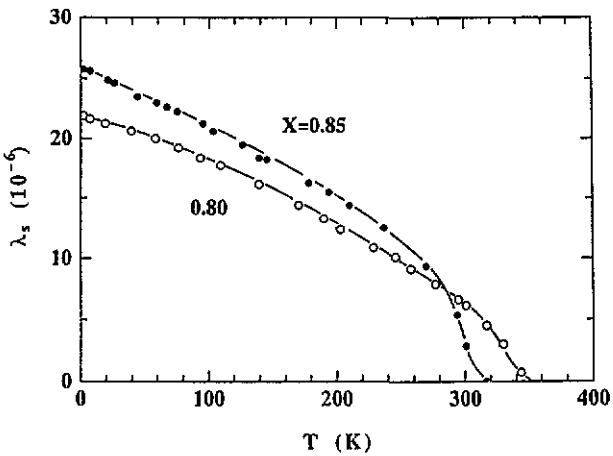

Figure 7. Temperature dependence of the saturation magnetostriction λ_s for the ferromagnetic amorphous La(Fe$_x$Al$_{1-x}$)$_{13}$ alloys with $x = 0.80$ and 0.85.

Fe^{I} atom. The magnitudes of the magnetic moments of these two sites are very different from each other. For example, the value for Fe^{I} is $1.1\mu_B$ and that for Fe^{II} is $2.14\mu_B$ for the crystalline La(Fe$_{0.91}$Al$_{0.09}$)$_{13}$ alloy (Helmholdt *et al* 1986). The present amorphous counterparts also have icosahedral clusters composed of Fe^{I} and Fe^{II} (Matsubara *et al* 1992, Chiang *et al* 1994). Therefore, the magnetic state of Fe^{I} would be different from that of Fe^{II}, resulting in interactions which follow the two-ion model.

Figure 11 shows the temperature dependence of the offset caused by the magnetic

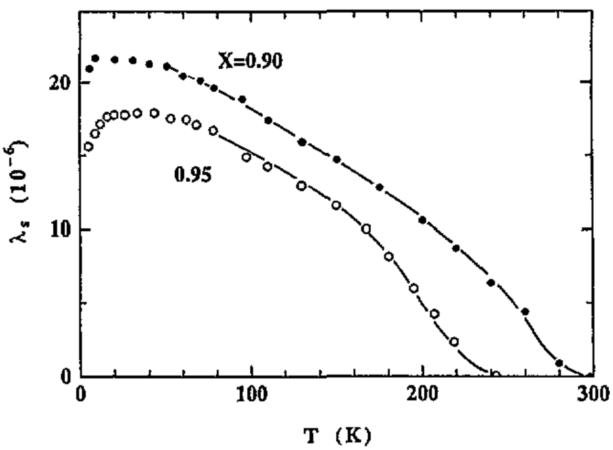

Figure 8. Temperature dependence of the saturation magnetostriction λ_s for the re-entrant spin-glass amorphous $La(Fe_xAl_{1-x})_{13}$ alloys with $x = 0.90$ and 0.95.

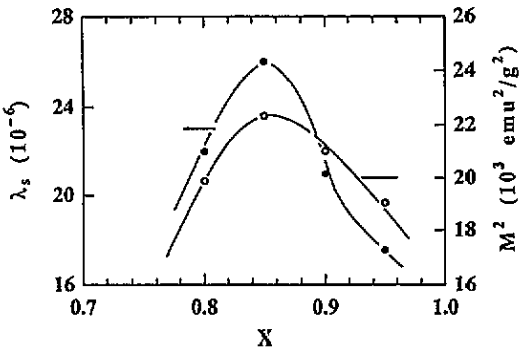

Figure 9. Concentration dependence of the saturation magnetostriction λ_s at 4.2 K in 10 kOe, together with that of the square M^2 of the magnetization (Chiang *et al* 1991) measured in the same applied magnetic field as for the amorphous $La(Fe_xAl_{1-x})_{13}$ alloys.

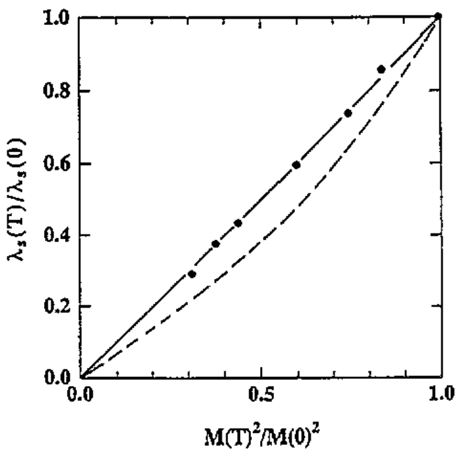

Figure 10. The saturation magnetostriction λ_s versus the square M^2 of the magnetization for the amorphous $La(Fe_{0.80}Al_{0.20})_{13}$ ferromagnetic alloy: – – –, one-ion model; ——, two-ion model.

viscosity $\Delta\lambda$ for the re-entrant spin-glass alloys. The value of $\Delta\lambda$ is defined by the value indicated in the inset which is a schematic figure around the origin for the re-entrant spin glass in figure 5. The directions of the arrows indicate increasing and decreasing applied magnetic fields. The transverse magnetostriction $\lambda_\perp$ does not return to the starting point when the applied magnetic field is reduced to zero. The value of $\Delta\lambda$ disappears in the vicinity of 20 K for $x = 0.90$ and 70 K for $x = 0.95$, as seen from figure 11. It is worth noting that these temperatures correspond to their spin freezing temperature in zero magnetic field as seen from figure 3. Therefore, it is concluded that this magnetic viscosity is caused by the spin-glass state.

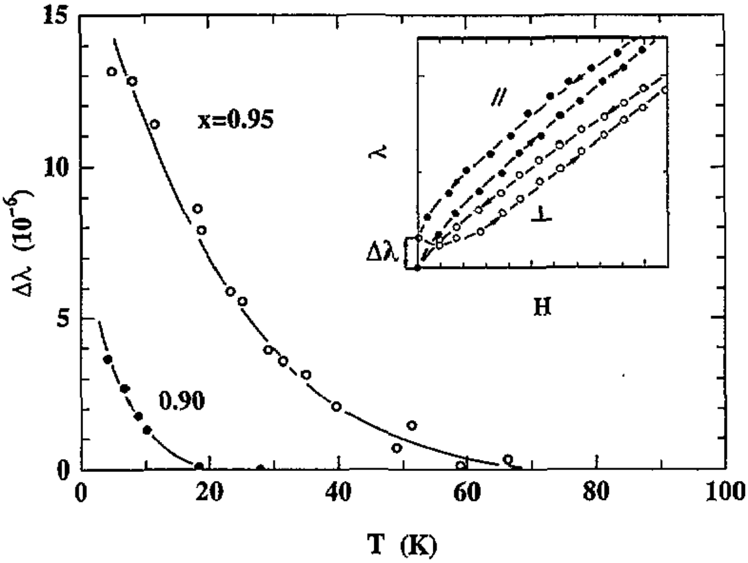

Figure 11. Temperature dependence of the offset for the linear magnetostriction $\Delta\lambda$ due to the magnetic viscosity for the amorphous $La(Fe_{0.90}Al_{0.10})_{13}$ and $La(Fe_{0.95}Al_{0.05})_{13}$ alloys. The inset shows the schematic figure to define the value of $\Delta\lambda$ in the vicinity of the origin for the re-entrant spin-glass alloys given in figure 5. The directions of the arrows indicate the increasing and decreasing applied magnetic fields.

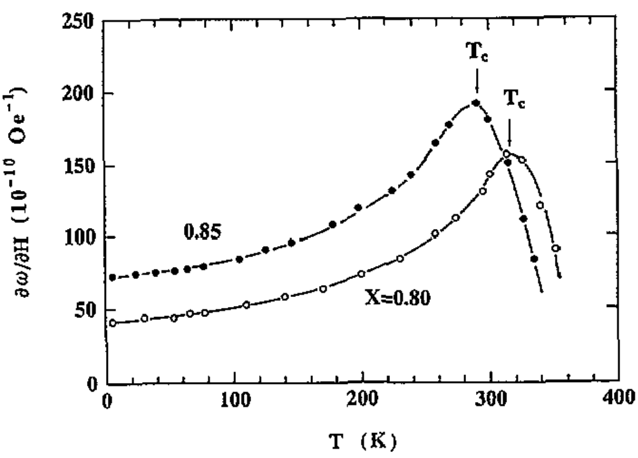

Figure 12. Temperature dependence of the forced-volume magnetostriction $\partial\omega/\partial H$ for the ferromagnetic amorphous $La(Fe_xAl_{1-x})_{13}$ alloys with $x = 0.80$ and 0.85.

Shown in figure 12 is the temperature dependence of the forced-volume magnetostriction $\partial\omega/\partial H$ for the ferromagnetic amorphous $La(Fe_xAl_{1-x})_{13}$ alloys with $x = 0.80$ and 0.85. The value of $\partial\omega/\partial H$ is obtained from the following equation:

$$\partial\omega/\partial H = (\partial\lambda/\partial H)_{\parallel} + 2(\partial\lambda/\partial H)_{\perp}. \tag{1}$$

These curves exhibit a peak at the Curie temperature T_C. The data for the re-entrant spin-glass amorphous $La(Fe_xAl_{1-x})_{13}$ alloys with $x = 0.90$ and 0.95 are also given in figure 13. The magnitudes of $\partial\omega/\partial H$ for both ferromagnetic and re-entrant spin-glass amorphous alloys are very large and comparable with those of amorphous Zr–Fe and Zr–Fe–Ni alloys (Tange *et al* 1989, 1990). Note that $\partial\omega/\partial H$ for α-Fe and γ-Ni at room temperature are 5×10^{-10} Oe^{-1} and 1×10^{-10} Oe^{-1}, respectively (Snoek 1937, Tange and Tokunaga 1969). The transition temperature T_f is affected by applying a magnetic field as seen from figure 3, but the variation in T_f is not so significant above several hundred oersteds. On the other hand, T_C is slightly increased, as mentioned before. Therefore, we can define these two temperatures as given by the arrows in figures 12 and 13. The peak at the Curie temperature T_C is reduced with increasing x and eventually disappears in the curve for $x = 0.95$.

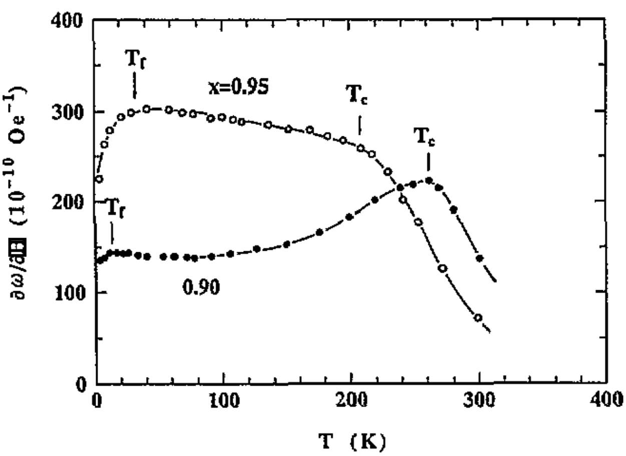

Figure 13. Temperature dependence of the forced-volume magnetostriction $\partial\omega/\partial H$ for the re-entrant spin-glass amorphous $La(Fe_xAl_{1-x})_{13}$ alloys with $x = 0.90$ and 0.95.

The forced-volume magnetostriction $\partial\omega/\partial H$ in the re-entrant spin-glass regime around amorphous Fe has been investigated on the basis of the finite-temperature theory of local environment effects for amorphous metallic magnetism (Kakehashi 1993). According to this theory, the peak at the freezing temperature is caused by the change in the amplitudes of local magnetic moments, which is characteristic of the itinerant-electron spin glasses. It should be emphasized that such a peak is hardly observed in the insulator spin glasses. Furthermore, this theory points out that the peak corresponding to the spin freezing temperature becomes clear with decreasing Curie temperature, whereas the peak at the Curie temperature becomes obscure. Therefore, the present results seem to be consistent with the theoretical considerations mentioned above.

Figure 14(*a*) shows the concentration dependence of $\partial\omega/\partial H$, together with that of the high-field susceptibility χ_{hf} (Chiang *et al* 1991). The data on the spontaneous volume magnetostriction ω_s (Chiang *et al* 1992) and the compressibility κ are given in figure 14(*b*). As is well known, the conventional expression of the forced-volume magnetostriction $\partial\omega/\partial H$ is given by the following expression:

$$\partial\omega/\partial H = 2\kappa CM\partial M/\partial H = 2\kappa CM\chi_{hf} \qquad (2)$$

where κC is the magnetoelastic coupling constant and $\partial M/\partial H = \chi_{hf}$ is the high-field susceptibility. On the other hand, in the theoretical model taking the thermal spin

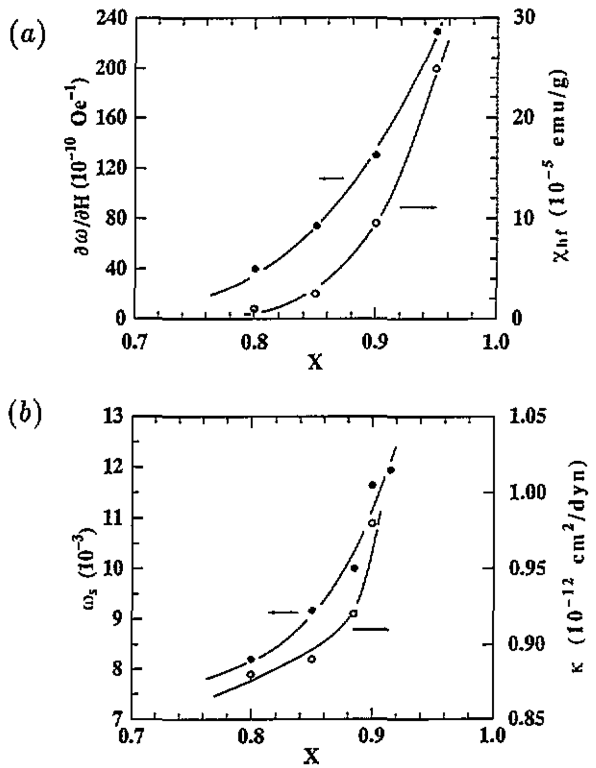

Figure 14. (*a*) Concentration dependence of the forced-volume magnetostriction $\partial\omega/\partial H$ for the La(Fe$_x$Al$_{1-x}$)$_{13}$ alloys, together with that of the high-field susceptibility χ_{hf} (Chiang *et al* 1991). (*b*) The data on the spontaneous volume magnetostriction ω_s (Chiang *et al* 1992) and the compressibility κ.

fluctuations into consideration, the forced-volume magnetostriction $\partial\omega/\partial H$ is calculated from the following equation (Kakehashi 1993):

$$\frac{\partial\omega}{\partial H} = \frac{\dot{D}\kappa}{V}\left(T\frac{\partial[\langle m\rangle]_s}{\partial T} + \frac{1}{4}\tilde{J}\frac{\partial[\langle\xi^2\rangle]_s}{\partial H}\right) \tag{3}$$

where V is the volume per atom, $\dot{D}$ is the proportionality constant given by the radial wavefunction at the Wigner–Seitz sphere, $\tilde{J}$ is the effective exchange energy parameter, $\langle\rangle$ and $[]_s$ indicate the thermal and structural averages, respectively, ξ is the site-dependent random exchange field and the amplitude $[\langle\xi^2\rangle]_s$ is directly connected with the amplitude $[\langle m^2\rangle]_s$ of the local magnetic moment. It has been pointed out that the second term in equation (3) is dominant in itinerant-electron spin glasses (Kakehashi 1993). From equations (2) and (3), the forced-volume magnetostriction $\partial\omega/\partial H$ is proportional to the compressibility κ.

The value of κ is obtained from the following conventional expression:

$$\kappa = 3(1-2\sigma)/E \tag{4}$$

where σ is Poisson's ratio and E Young's modulus. These two values at room temperature have been obtained from the Brillouin scattering data (Yoshihara *et al* 1994). On the other hand, the temperature dependence of E for the amorphous La$(Fe_xAl_{1-x})_{13}$ alloys is available (Chiang *et al* 1992). Therefore, we can obtain the compressibility κ at 4.2 K from these results for the present amorphous alloys. The value of κ thus obtained is very large, ranging from 0.88×10^{-12} to 0.98×10^{-12} cm^2 dyn^{-1} in the range $0.80 \leqslant x \leqslant 0.90$, being about twice that of the crystalline α-Fe, as shown in figure 14(*b*). Therefore, the large values of $\partial\omega/\partial H$ given in figures 12 and 13 are closely correlated with such a large value of κ. These results on $\partial\omega/\partial H$, χ_{hf}, κ and ω_s show similar trends. Recently, RE$(Fe_xAl_{1-x})_{13}$ (RE $\equiv$ La, Y, Ce or Lu) amorphous alloys consisting of the icosahedral clusters have been confirmed as exhibiting re-entrant spin-glass behaviour in higher Fe concentration ranges above $x = 0.90$ (Fukamichi *et al* 1994). The forced-volume and saturation magnetostrictions of these amorphous alloys are also expected to be similar to those of the present amorphous alloys.

4. Conclusion

The dependences of saturation and forced-volume magnetostrictions on concentration and temperature have been investigated for the amorphous La$(Fe_xAl_{1-x})_{13}$ alloys prepared by high-rate DC sputtering. Various physical values are closely interrelated with their significant magnetovolume effects. These results have been discussed in connection with the magnetic phase diagram obtained from the differential magnetic susceptibility $\mathrm{d}M/\mathrm{d}H$. Furthermore, the itinerant spin-glass behaviour has been discussed. The main results are summarized as follows.

(a) In the re-entrant spin-glass regime, the Curie temperature T_C is slightly increased but the spin freezing temperature T_f is drastically decreased on application of a magnetic field.

(b) The magnetic field dependence of the saturation magnetostriction λ_s in the spin-glass state exhibits hysteresis which disappears above the spin freezing temperature T_f.

(c) The concentration dependence of the saturation magnetostriction λ_s is similar to that of the square M^2 of the magnetization.

(d) The temperature dependence of the saturation magnetostriction λ_s for the amorphous ferromagnetic alloys is explained by the two-ion model.

(e) The forced-volume magnetostriction $\partial\omega/\partial H$ for the re-entrant spin-glass alloys exhibits a broad peak at the spin freezing temperature T_f in addition to the peak at the Curie temperature T_C.

(f) The peak at the spin freezing temperature T_f is explained to be characteristic in the itinerant-electron spin glass. The giant forced-volume magnetostriction $\partial\omega/\partial H$ is associated with the itinerant-electron spin-glass state.

(g) The value of $\partial\omega/\partial H$ at 4.2 K shows a marked increase with increasing Fe concentration, in analogy with the spontaneous volume magnetostriction ω_s, the compressibility κ and the high-field susceptibility χ_{hf}.

Acknowledgments

The support by grant-in-aid for scientific research (A) 04402045 from the Japanese Ministry of Education, Science and Culture is gratefully acknowledged. We thank Professor E Matsubara of Kyoto University, Professor Y Waseda of the Institute for Advanced Materials Processing, Tohoku University, and Dr A Yoshihara of the Research Institute for Scientific Measurements, Tohoku University, for many helpful discussions and suggestions during the present work.

References

Berry B S and Pritchet W C 1978 *Solid State Commun.* **26** 827–9
Callen E R and Callen H B 1963 *Phys. Rev.* **120** 578–93
—— 1965 *Phys. Rev.* A **139** 455–71
Chiang T H, Fukamichi K and Goto T 1992 *J. Phys.: Condens. Matter* **4** 7489–98
Chiang T H, Fukamichi K, Komatsu H and Goto T 1991 *J. Phys.: Condens. Matter* **3** 4055–55
Chiang T H, Matsubara E, Kataoka N, Fukamichi K and Waseda Y 1994 *J. Phys.: Condens. Matter* **6** 3459–68
Fujita A, Komatsu H, Fukamichi K and Goto T 1993 *J. Phys.: Condens. Matter* **5** 3003–10
Fukamichi K 1983 *Amorphous Metallic Alloys* ed F E Luborsky (London: Butterworths) pp 317–40
Fukamichi K, Chiang T H, Ohashi N, Kataoka N, Matsubara E, Waseda Y and Goto T 1994 *Mater. Sci. Eng.* A **181–2** 860–3
Fukamichi K, Goto T, Komatsu H and Wakabayashi H 1989 *Proc. 4th Int. Conf. on the Physics of Magnetic Materials* ed W Gorzkowski, H K Lachowicz and H Szymczak (Singapore: World Scientific) pp 354–81
Fukamichi K, Kikuchi M and Masumoto T 1984 *J. Non-Cryst. Solids* **61–2** 961–6
Helmholdt R B, Palstra T T M, Nieuwenhuys G J, Mydosh J A, van der Kraan A M and Buschow K H J 1986 *Phys. Rev.* B **34** 169–73
Hiroyoshi H and Fukamichi K 1982 *J. Appl. Phys.* **53** 2226–8
Kakehashi 1993 *Phys. Rev.* B **47** 3185–95
Kofart D D, Nanao S, Egami T, Wong K M and Poon S J 1986 *J. Appl. Phys.* **57** 114–7
Ludorf W, Abd-Elmegnid M M and Micklitz H 1989 *J. Magn. Magn. Mater.* **78** 171–5
Matsubara E, Waseda Y, Chiang T H and Fukamichi K 1992 *J. Mater. Eng. Lett.* **11** 1521–4
O'Handley R C 1977 *Solid State Commun.* **21** 1119–22
—— 1978 *Phys. Rev.* B **18** 930–8
Palstra T T M, Nieuwenhuys G J, Mydosh J A and Buschow K H J 1984 *J. Appl. Phys.* **55** 2367–9
—— 1985 *Phys. Rev.* B **31** 4622–32
Palstra T T M, Nieuwenhuys G J, Mydosh J A, Helmholdt R B and Buschow K H J 1986 *J. Magn. Magn. Mater.* **54–7** 995–6
Shiga M 1992 *Electronic and Magnetic Properties of Metals and Ceramics* Part II, ed K H J Buschow (Weinheim: VCH) pp 159–210
Snoek J L 1937 *Physica* **4** 853–62
Tange H, Kamimori T, Goto M and Fukamichi K 1990 *J. Magn. Magn. Mater.* **90–1** 335–6
Tange H, Tanaka Y, Goto M and Fukamichi K 1989 *J. Magn. Magn. Mater.* **81** L243–6
Tange H and Tokunaga T 1969 *J. Phys. Soc. Japan* **27** 789
Wassermann E F 1990 *Ferromagnetic Materials* vol 5, ed K H J Buschow and E P Wohlfarth (Amsterdam: North-Holland) pp 237–322
Widom M 1988 *Introduction to Quasicrystals* ed M V Jarić (London: Academic) pp 59–110
Yoshihara A, Shimada Y, Chiang T H and Fukamichi K 1994 *J. Appl. Phys.* **75** 1733–8